Thermal-Cycling-Induced Spectral Diffusion and Thermal Barriers in Anisole-Doped Cyclohexane, an Unusual Multiphase Host−Guest System†

Mark M. Somoza* and Josef Friedrich

Physik Department E14, Lehrstuhl für Physik Weihenstephan, Technische Universität München, An der Saatzucht 5, D-85350 Freising, Germany

Received: September 14, 2005; In Final Form: December 27, 2005

The host−guest system of anisole incorporated into a cyclohexane matrix was investigated in a series of hole-burning experiments. This system is unusual in that cyclohexane can freeze into coexisting solid phases. The hole-burning experiments support the existence of two crystalline phases and one disordered phase. A second surprising characteristic of this system is that the quasi-line absorption features of the spectra appear inverted at low temperature because of unexpected dominance of fluorescence and phosphorescence.

Introduction

Persistent spectral hole burning is a very sensitive technique for investigating structural changes in materials such as glasses,[1−6] proteins,[7−10] polymers,[11−14] and crystals.[15−19] Structural changes may be induced by a variety of external influences, for instance, changes in temperature[20−22] and pressure.[23−28] When a narrow spectral hole is burned into the low-temperature absorption spectrum of the sample, via a laser-induced photoreaction, the hole becomes a marker or label of the initial structural state. Subsequent structural changes are reflected in changes in the area, shape, or spectral position of the hole.

The case when the temperature is the environmental variable and is varied after the initial hole-burning process will be discussed here. An increased temperature provides the system with additional energy to explore a larger region of its structural phase space. Thus, the original hole broadens with increased temperature. If the hole recovers its original shape when cooled back to the starting temperature, the system has returned to its original configuration. Irreversible changes to the hole, however, are likely and can be resolved into two independent parameters, hole area and hole broadening. Since the absorption hole area is directly proportional to the number of phototransformed chromophores, a change in area upon cooling to the starting point after a temperature excursion indicates a thermally induced back-reaction that partially erases the effect of the hole burning. The height and width of this thermal barrier separating product and educt states can be resolved by repeated excursions to gradually increasing temperatures.[29]

Spectral diffusion, as measured by the broadening of the hole observed after the sample is subjected to a temperature excursion, is a measure of ergodicity of the system, that is, the ability of the system to find its structural equilibrium. The original hole marks the structural configuration that was originally frozen in upon cooling to the hole-burning temperature. Subsequent spectral diffusion, upon thermal cycling, indicates that the system was not at equilibrium and that other areas of configuration space are also local minima and are accessible with the energy provided during the thermal cycle.

Glasses and crystals are generally regarded as opposing archetypes from the perspective of spectral diffusion. Glasses are structurally disordered and are far from equilibrium whereas crystals are ordered and at equilibrium. The structural phase space of glasses is usually modeled as an ensemble of a two-level system (TLS) with a distribution of energies and barriers.[30,31] The TLS framework at least qualitatively explains many of the differences in physical properties between glasses and crystals.[32] The TLS model suggests that spectral diffusion broadening of holes with temperature is governed by a power law with an exponent close to 1.[33−35] Spectral diffusion in crystals has received little attention because the reasonable expectation is that there should not be any spectral diffusion in crystals. An ideal crystal will always relax to its single equilibrium configuration. Nevertheless, a handful of studies have looked at the effects of thermal cycling on spectral diffusion in crystals and have indicated that the effect is significantly smaller than is observed in glasses but is definitely present.[18,25]

Here, we report on hole-burning and thermal-cycling experiments in anisole doped at low concentrations into a cyclohexane host matrix. At low temperatures, this system consists of both crystalline and glassy domains. The glassy domains lead to a broad background in the absorption spectrum that closely resembles the room-temperature (liquid) spectrum. The crystalline domains contribute sharp quasi-lines to the absorption spectrum. An unexpected characteristic of this system is that at low temperatures the spectra due to anisole molecules incorporated into the crystalline phases appear as inverted absorption spectra. Figure 1 shows this interesting effect. The room-temperature absorption spectrum is the dashed line and includes negligible contribution from fluorescence or phosphorescence. The upper solid line is a 43 K absorption spectrum and clearly shows the contributions from both the crystalline and amorphous domains. This spectrum is weakly contaminated by reemitted photons and is a qualitative representation of the absorption spectrum at this temperature. The lower solid line is from data taken at 4.2 K and appears as an inverted absorption spectrum because the signal detected at the quasi-line wavelengths is dominated by fluorescence and phosphorescence photons. Because the low-temperature spectra in this system are strongly influenced by contributions from luminescence, the label log P_0/P is used instead of absorbance, where P_0 and P are, respectively, the incident and the detected (vs transmitted) radiant power. A more detailed description of the spectral inversion process is given in ref 36. We will argue later in this

† Part of the special issue "Robert J. Silbey Festschrift".

* To whom correspondence should be addressed. E-mail: Mark.Somoza@physik.blm.tu-muenchen.de.

10.1021/jp055194p CCC: $33.50
Published on Web 02/04/2006

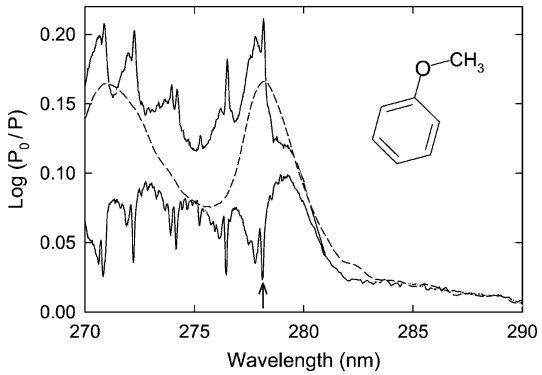

Figure 1. Spectrum of anisole in a cyclohexane host matrix (10^{-4} M/M, 0.5-mm path length) at three different temperatures: 300 K (dashed line), 43 K (upper solid line), and 4.2 K (lower solid line). The quasi-line spectrum inverts at 33 K. Inset: structure of anisole. The arrow indicates the hole-burning wavelength.

paper that the interaction of anisole with one of the crystalline phases of cyclohexane observed in the thermal-cycling experiments is correlated to the spectral inversion.

Experiment

Anisole and cyclohexane were obtained from Sigma-Aldrich and were used without further purification. No trace of impurities was found in their absorption spectra. The data presented here is from a 1×10^{-4} mole ratio (M/M) dilution of anisole in cyclohexane in a poly(tetrafluoroethylene) sample cell with fused silica windows. The path length was 0.5 mm for the broad-band spectra and 2 mm for the hole-burning experiments. At this concentration of anisole, the low-temperature spectra, both from the amorphous phase and from the crystalline phase, are from isolated molecules. No shifting of the absorption spectra of these phases was observed relative to a room-temperature spectrum of a very dilute sample. Room-temperature absorption data was obtained in a Shimadzu spectrophotometer as well as in the same (uncooled) helium flow cryostat used for the low-temperature measurements. For the low-temperature measurements, the sample was initially cooled by insertion into the cold cryostat. Because the low-temperature properties of the sample depend on the initial cooling rate, this rate could be slowed by lowering the sample gradually into the cryostat or by inserting the sample into a warmer cryostat. Very fast quenching of the sample was possible by filling the sample chamber with liquid helium and inserting the sample quickly. We use "fast cooling" specifically to mean a transition time between room temperature and liquid helium temperature of about 30 s and "slow cooling" for a transition time of 1−2 min.

For experiments below 42 K, the sample temperature was measured with a germanium resistance thermometer and was regulated with a PID controller coupled to a sample chamber heater. At higher temperatures, a carbon or platinum resistance thermometer was used. Temperature regulation at the higher temperatures was by manual adjustment of cold helium gas flow into the sample chamber. The temperature accuracy was better than 0.2 K below 20 K, better than 0.5 K below 40 K, and better than 1 K at higher temperatures.

The light source for the hole-burning and scanning experiments was a Coherent 899-21 actively stabilized ring laser (500 kHz line width) operating with Rhodamine 110 and adapted to long-range scans with a Coherent Autoscan external controller. The output of the ring laser was frequency doubled by a BBO crystal in an external resonator that actively tracked the laser frequency (LAS Wavetrain SC). The UV output from this resonator was coupled to the cryostat optics with a multimode optical fiber. The fiber was mechanically shaken with a modified fish-tank air pump to prevent speckle noise.[37] The output from the fiber was recollimated and filtered (Schott BG 24) to remove remaining traces of the fundamental as well as fiber fluorescence. Neutral density filters were used to attenuate the light intensity to a level appropriate for hole burning. For scanning, the intensity was attenuated by an additional 3 orders of magnitude. Light for the reference channel was sampled with an uncoated piece of fused silica and was focused into a detector. The remaining light was focused into the sample. Light transmitted from the opposite side of the sample was collected with a lens close to the exit window of the cryostat and was focused onto the detector with a second lens. The solid angle of collection of light for the signal channel was 0.4% of 4π steradians. Light in both signal and reference channels was measured with Hamamatsu R928 photomultiplier tubes (PMT). These detectors have an almost flat quantum efficiency curve throughout the region of absorption and luminescence of the sample. When scanning with the laser, a 10-nm band-pass filter centered at 280 nm was used before the signal PMT to remove a large fraction of the luminescence signal.

Broad-band absorption and excitation spectra were obtained with the exact same setup, except that the light source was a monochromator with a spectral resolution set to 0.08 nm and was illuminated by a xenon short-arc lamp. Data for background subtraction was obtained from a pure cyclohexane sample frozen to 4.2 K. The blank sample had no absorbance in the range of the experiments and had a spectrally neutral light-scattering profile between 270 and 500 nm, the full range of the absorption measurements and luminescence from the sample. Outside the absorption band, low-temperature transmission through the frozen sample was weakly dependent on temperature, increasing by about 3.5% between 4 and 50 K.

Thermal-Cycling Method. All thermal-cycling experiments were carried out on holes burned at 279.2 nm, close to the peak of the most prominent zero-phonon quasi-line. The sample temperature during burning was 4 K. The sample was irradiated with a laser power of approximately 10 μW for 30 min. The illuminated sample volume was approximately 10 mm^3. The laser power used was comparatively low, but no effort was made to burn the holes close to the homogeneous line width as only changes to the holes are evaluated with this methodology and a sufficient starting area is necessary to obtain accurate results after cycling to high temperatures.

Immediately after burning, the laser power was attenuated by a factor of 1000 and was used to take a spectrum of the resulting hole. The spectral resolution of the scans was 50 MHz. After recording the hole, the sample temperature was increased to the excursion temperature and was allowed to remain at this temperature for about 15 min. The time required to reach the excursion temperature depended strongly on the temperature difference and ranged between 5 min for the 7 K data point and 15 h for the 100 K data point. After the 15 min equilibration time at the excursion temperature, the sample was cooled to 4 K and was rescanned. This process was repeated for each of the excursion temperatures. For each spectrum, the area and spectral width of the hole was obtained by fitting the data to an appropriate line shape (see below).

Results

I. Hole Recovery. Spectral holes can be easily burned into the spectral region of the principle quasi-line at 277.9 nm. The recovery of holes with thermal cycling will be examined in this section.

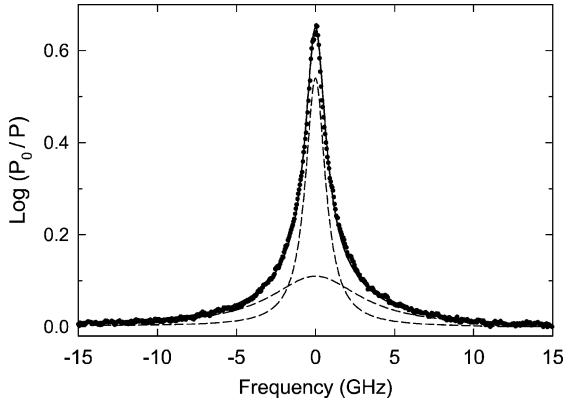

Figure 2. Original hole burned at 4.2 K at 277.92 nm before thermal cycling. The hole is fit to the sum (solid line) of two Lorentzians with distinctly different widths (dashed lines). The narrow Lorentzian component of the hole does not contribute to the area after thermal cycling to 12 K.

The change in hole area during thermal cycling is independent of the model used to fit the line shape as long as the fit accurately represents the area. Nevertheless, here we have fit the holes with the sum of two Lorentzians. This fit was chosen because it accurately represents the shape of the holes, but more importantly, because the data suggest that hole burning and recovery is distributed between two distinct ensembles of anisole environments. Widths derived from these same fits will be used in the next section to interpret spectral diffusion in this sample. The recovery of the hole can then be resolved into the recovery of each of these species. Figure 2 shows the original hole burned at 4 K before any thermal excursions. The hole is fit by the sum of a narrow and a wide Lorentzian. The sum of these Lorentzians also accurately represents the shape of the hole after all subsequent cycles although the narrow Lorentzian does not contribute to the line shape after excursions beyond 12 K.

The results of thermal cycles on hole area is shown in Figure 3. The filling of the hole has been normalized to the area of the initial hole. The thermal recovery pattern has been resolved into separate recoveries of the wide and the narrow Lorentzian in addition to the total area recovery. The fits for the area recovery data are based on the assumption of a Gaussian distribution of barriers between product and educt states. The area remaining after each thermal cycle is then one minus the cumulative distribution function evaluated at the excursion temperature. The Gaussian distributions responsible for each of the area fits are shown at the bottom of Figure 3. Most of the hole area recovers in two steps, with the remaining hole area persisting to temperatures well above 100 K. The narrow Lorentzian component recovers completely at a Gaussian barrier with a mean μ of 11 K and a standard deviation σ of 1.3 K. The recovery curve for the wide Lorentzian is well described by a bimodal Gaussian distribution with the higher temperature barrier dominating the total recovery. The low-temperature barrier ($\mu = 12.5$ K, $\sigma = 1.5$ K) is quite similar to the narrow Lorentzian barrier, but the higher temperature barrier ($\mu = 33$ K, $\sigma = 3.5$ K) is distinct. The distribution of data points in the vicinity of this second barrier is insufficiently dense for an unambiguous fit and the exact values have been chosen to match a much denser data series presented below.

The reversal of the broad-band spectra at temperatures corresponding to the second barrier observed in the thermal-cycling experiments suggests a correlation. To examine the connection between the two observations, the integrated intensity detected within the peak of the principle quasi-line at 277.9 nm was taken as a proxy of the spectral inversion of the slow-cooled sample and was plotted as a function of sample temperature. The results are shown in Figure 4. As the distribution of points suggests a cumulative distribution function similar to those in Figure 3, an identical fitting procedure was used and results in a Gaussian distribution centered at 33 K with a standard deviation of 3.5 K.

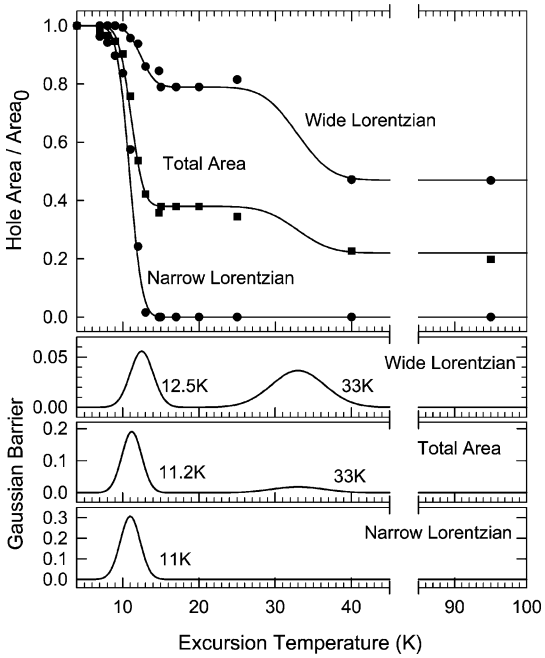

Figure 3. Decay of the hole area upon thermal cycling. The hole has been fit with the sum of a wide and a narrow Lorentzian. The fits to the hole area of each Lorentzian, as well as their sum (top graph), are based on Gaussian distributions of barrier heights. The bottom graph shows the Gaussians that lead to the observed hole decay.

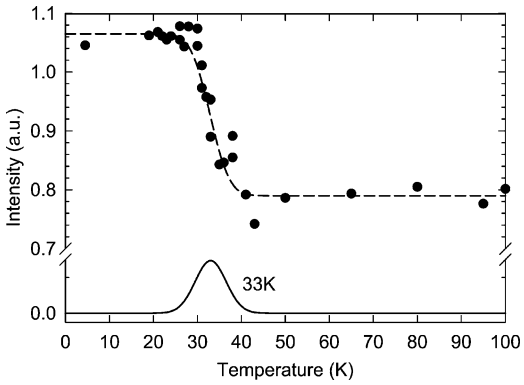

Figure 4. Inversion of the spectrum ("slow-cooling" sample) with temperature on the basis of the intensity of the peak of the 277.9-nm quasi line (circles). The data have been fit on the basis of the assumption of a Gaussian distribution of structural barriers separating the normal and inverted spectra (dashed line). The lower plot shows the actual Gaussian ($\mu = 33$ K and $\sigma = 3.5$ K) and is plotted with an arbitrary amplitude.

II. Spectral Diffusion. The broadening of the spectral holes was determined from the thermal-cycling data by extracting the widths of the two Lorentzians used to fit the data. We emphasize that spectral diffusion information, although obtained from the same fits used to determine area recovery, is due to an independent physical process. Figure 5 shows the spectral diffusion behavior for the two population subsets represented by the narrow and the wide Lorentzians. The vertical axis is the full width at half-maximum Γ measured at 4.2 K. The narrow Lorentzian does not contribute area to the hole past 12 K.

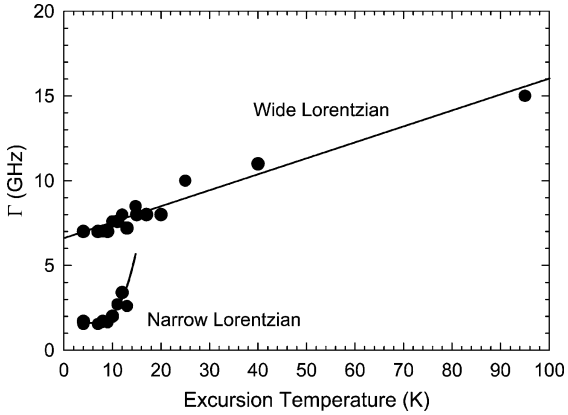

Figure 5. Broadening of the two Lorentzian components of the hole under thermal-cycling conditions. The wide Lorentzian broadens linearly with temperature while the narrow Lorentzian broadening is consistent with a power law with an exponent of 3.5.

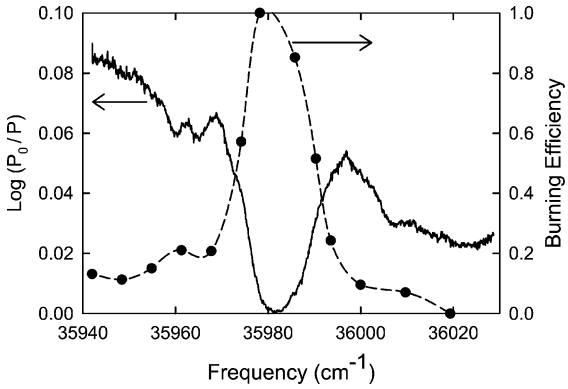

Figure 6. Efficiency of persistent hole burning in the vicinity of the 277.9-nm quasi-line. Each circle represents the relative area of a hole burned at a fixed laser power and burning time. The efficiency spline curve (dashed line) is superimposed on the spectrum of the same region.

Nevertheless, it is clear from this limited range that spectral diffusion of this component can be described by a power law behavior with an associated exponent close to 3.5. The wide Lorentzian persists to the highest temperatures attempted and throughout the range its broadening is well described by a line with slope 0.14 GHz/K.

It is clear from both the area-filling data in Figure 3 and the hole broadening in Figure 5 that the two Lorentzian fits are justified and therefore that there are two distinct populations represented in the quasi-line that are addressed by the laser-burning process.

Discussion

I. Structural Polymorphism. The data presented here indicate that anisole interacts with three distinct structural phases of cyclohexane. An amorphous phase is observed at all temperatures below room temperature; in addition, a series of quasi-lines, attributed to crystalline phases, are seen below 100 K. Within the crystalline domains, the hole-burning experiments identify two distinct crystalline phases.

Although the specific photoreaction that leads to hole burning in this system is not known, the experiments provide strong evidence that the reaction is environmentally mediated. Hole burning was not possible or was multiple orders of magnitude weaker in the glassy domains (see Figure 6). This suggests that the hole-burning mechanism is photophysical rather than photochemical, as photochemical reactions are rather less sensitive to the particular arrangement of neighboring host molecules. Dimethyl-s-tetrazine (DMST), for example, undergoes an efficient and irreversible photochemical dissociation as a guest in a variety of crystal and glass hosts.[15,39] A candidate for a photophysical mechanism is a photoinduced reorientation of the guest within the host matrix, in particular, a reorientation of the methoxy group between conformations with different transition energies. The photoreorientation leads to less absorption at the burning frequency. Area recovery during thermal cycling reflects the return to the original low-energy position that was frozen in during the original crystallization. Because anisole is slightly larger than cyclohexane, the crystalline domains may contain anisole replacing two adjacent cyclohexane sites in the lattice. Reorientation would take place within this space, possibly aided by a reorganization of host molecules in adjacent lattice sites. Anisole incorporated into the glassy phase may encounter higher reorganization barriers or more efficient dissipation of the photon energy.

It is known, principally from Raman experiments, that cyclohexane undergoes a solid−solid phase transition at 186 K.[40] The crystalline phase above this transition (solid I) is a cubic plastic crystal; that is, the centers of mass of the molecules form a crystal but the individual molecules have no rotational order or are subject to only weak orientational barriers. A transition to a true crystalline phase takes place below 186 K (monoclinic solid II). However, rapid cooling or quenching from the liquid phase or from the plastic crystal phase to below 186 K leads to a mix of solid II and a metastable phase distinct from solid II. This metastable phase has been characterized as a plastic crystal glass.[41,42] More recent studies, however, have disputed this finding and characterize this phase as an orientationally ordered state similar to one of the high-pressure phases (solid IV).[43−45]

Solid II of cyclohexane may be the phase which gives rise to the wide Lorentzian in the hole-burning experiments. According to the Raman experiments, this is the predominant crystalline phase below 186 K. Solid IV is the remaining low-temperature phase and is presumably responsible for the narrow Lorentzian hole. Both the wide and the narrow Lorentzians show a very similar area recovery pattern near 12 K. This suggests that crystalline phases associated with each Lorentzian are also structurally very similar, in general agreement with the similarities in the Raman spectra among the various identified cyclohexane phases.[44]

II. Irreversible Line Broadening. Spectral diffusion is the result of a dispersion of the host−guest configurations. The hole-burning process labels the initial distribution of interactions, and the subsequent line broadening reflects a redistribution of the dye-lattice couplings among the molecules spectrally adjacent to the hole. There are two common types of spectral diffusion experiments. Time-dependent experiments monitor the width of the hole as a function of waiting time after burning, whereas temperature-cycling experiments monitor the width of the hole as a function of excursion temperature. The techniques are approximately equivalent in that they both explore the same energy landscape, but temperature cycling, as an activating process, surveys the landscape with some power of temperature rather than logarithmically in time.

During the thermal-cycling experiments, two processes are taking place simultaneously. The area of the hole decays because absorber molecules that were "burned" return to their original spectral location. The width of the hole also broadens because neighboring "unburned" absorber molecules diffuse in the host−guest interaction space and find lower energy configurations. In this second case, the hole broadens but the area does not

change because the number of unburned absorbers stays constant. These two processes are independent because they depend on two distinct populations: burned and unburned. The hypothesis that the two processes are experimentally independent is based on the assumption that the structural barriers separating the photoproducts from their original state are quite different from the energy barriers separating alternative host−guest interactions. That this hypothesis is correct for the data presented here is easily seen by comparing Figures 3 and 5. Figure 3 shows that there are two well-defined structural barriers between educt and photoproduct. Figure 5, particularly the wide Lorentzian plot, shows that the structural relaxation barriers are continuously distributed and that there are no special contributions to the width at the two area recovery temperatures (12.5 and 33 K). In the case of the narrow Lorentzian, this conclusion is less definite because of the intrinsically limited data range due to complete area recovery at low temperatures.

That spectral diffusion occurs at all in crystalline domains suggests that, at least with a sufficiently sensitive measurement, the structure and long-range order associated with crystals is not in thermodynamic equilibrium. Spectral diffusion has been observed in certain exceptional pure and doped molecular crystals where the guest can induce disorder or where two-level systems are generated by mobile protons in hydrogen bonds or by the mobility of coupled methyl groups.[46,47] The distribution of configurational barriers, as reflected in the smooth line broadening behavior of Figure 5, is continuous and unstructured. This pattern is quite similar to the spectral diffusion behavior that is observed and expected in glasses. In glasses, the irreversible spectral diffusion during thermal cycling can be modeled as a superposition of tunneling processes (which lead to linear broadening in temperature T) and thermally activated barrier crossings ($\sim T^{3/2}$).[20] Experimentally, spectral diffusion in glasses has usually been fitted with a power law curve with an exponent value between 1 and 3. In the crystalline phases of anisole in cyclohexane, we have measured exponents of 3.5 and 1.0, values which seem quite glasslike. These values are also not so different from those reported for spectral diffusion in tertiary butyl-phthalocyanine doped *n*-octane, another crystalline system; these experiments lead to exponents of 2.4 and 2.8 for two different burning sites.[48]

Even though the spectral diffusion pattern is surprisingly glasslike, other experimental observations are completely consistent with what is expected from crystalline domains. The pattern of weakly inhomogeneously broadened quasi-lines must result from the dye embedded in only a few, well-defined crystalline lattice sites (Figure 1). The pattern of area recovery (Figure 3) is sharply structured, as opposed to the pattern observed in glasses, where the area recovers following a continuous distribution of barriers.

The glass-crystal duality of the observations suggests the following interpretation. The anisole molecule replaces one or more cyclohexane molecules in the cyclohexane crystalline matrix. Because of the constraints of the lattice, the local environment is well-defined and results in the spectrum of quasi-lines. The hole-burning photoreaction forces the anisole molecule into a metastable conformation within the lattice site. Because the structural barriers between photoproduct and educt are due to well-defined lattice−guest interactions, area recovery takes place over a narrow temperature range. In the case of the wide Lorentzian hole, there is a bimodal recovery, but both barrier distributions are quite narrow. The magnitude of the glasslike spectral diffusion suggests that the disorder cannot be attributed to the crystalline lattice or to guest-induced disorder and must originate from disordered domains in the sample. The disorder may originate in the domains of matrix-excluded anisole molecules that give rise to the broad background in the spectra. Spectral diffusion that may be taking place in these domains is then coupled to the crystalline lattice via a long-range strain field. In this model, the disorder in the matrix-excluded anisole domains results in an initial distribution of internal stresses that propagate through the medium primarily as elastic dipole−dipole interactions.[49] As a result of thermal cycling, the disordered domains partially relax and the strain field changes. The crystalline sites therefore participate in the spectral diffusion of the glassy sites by means of this coupling, albeit in an attenuated form because of the limited range of the elastic dipole ($1/r^3$) and shielding by intervening elastic deformations.

III. Hole Recovery. Hole recovery under thermal-cycling conditions measures the distribution of barriers separating the product state from the original state. That this process is completely independent from spectral diffusion dynamics has been discussed in the preceding section on the basis of the very different distribution of relaxation barriers observed for the two processes.

The hole recovery pattern has been separated into two components labeled as narrow Lorentzian and wide Lorentzian. This division is based on the observation that, at the lowest temperatures, the best fit for the hole is the sum of two Lorentzians with different widths. This fitting choice is reinforced by the fact that at higher temperatures a single Lorentzian is sufficient to describe the shape of the hole. This suggests that there are two populations of anisole environments that are addressed in the hole-burning process, one of which fully recovers at low temperature. In addition, at much lower laser power, single narrow Lorentzian holes are created, reinforcing the idea of a higher educt−product barrier for the wide Lorentzian. Finally, separating the hole shape into these two components results in two simple spectral broadening fits (Figure 5), a straight line for the wide Lorentzian and a power law for the narrow Lorentzian, rather than the more complex and composite spectral diffusion curve that results when the hole is treated as originating in a single population. Two distinct populations of anisole at the same burning site imply that the quasi-line where the burning takes place is actually composed of two overlapping zero-phonon lines. Figure 6 shows that this is a reasonable assumption. The burning efficiency curve in this figure appears to be decomposable into a narrow peak centered in the middle of the graph and a wide peak displaced a few wavenumbers toward lower energy. The overlap of two zero-phonon lines can be attributed to the structural similarity of the low-temperature cyclohexane phases II and IV.[44]

The bimodal Gaussian distribution of barriers for the wide Lorentzian hole (Figure 3) indicates that the photoreaction leads to two different kinds of product, one which recovers near 12 K and the other which recovers near 33 K. In addition, the wide component of the hole does not fully recover, even when the sample temperature is cycled up to 100 K. The incomplete recovery implies that there is at least one unobserved structural barrier above 100 K which accounts for nearly one-half of the unfilled area of the wide Lorentzian hole. Alternatively, there may be a separate reaction leading to an irreversible photochemical product state. The presence of multiple product states is surprising since the solvent cage of this cyclohexane phase must then be sufficiently complex to stabilize all of the photoproduct configurations with distinct and narrow barriers.

IV. Inversion. The spectral inversion that is observed in Figure 1 is due to anomalously high low-temperature absorption of anisole incorporated in the crystalline phase of the cyclohexane host matrix. That the host−guest interaction plays an important role is apparent from the effect of the initial sample cooling rate on the appearance of the spectral inversion. Fast cooling results in a spectrum where the quasi-lines appear inverted as soon as they become visible near 90 K (see ref 36 for the fast cooling spectrum and a more detailed discussion), whereas with slower cooling the absorption spectrum is normal at higher temperatures but inverts near 33 K (Figures 1 and 4). The behavior suggests the unfreezing of an activated process at this temperature. The methoxy group torsion is the softest mode and results in out-of-plane distortions that increase the nonradiative decay rate.[38] Low temperatures presumably favor the planar conformation, leading to increased emission and a larger intrusion of the excitation spectrum into the absorption spectrum.

Summary

Hole burning in a quasi-line of anisole-doped cyclohexane reveals that there are two distinct low-temperature crystalline phases in addition to the amorphous phase observed directly from the spectra. The two crystalline phases may be solids II and IV that have been previously detected in Raman experiments.

The hole recovery takes place with the well-defined steps expected in crystalline domains although the number of filling steps is surprising. Although spectral diffusion has been observed previously in crystals, the extent and pattern of the spectral diffusion, similar to that observed in glasses, suggests an elastic coupling between the crystalline and the glassy domains.

Acknowledgment. This work was made possible by financial support from the Deutsche Forschungsgemeinschaft (SFB 533 B5, FOR 358/2-A1) and from the Fond der Chemischen Industrie.

References and Notes

(1) Kharlamov, B. M.; Personov, R. I.; Bykovskaya, L. A. *Opt. Commun.* **1974**, *12*, 191.
(2) Haarer, D.; Silbey, R. *Phys. Today* **1990**, *43*, 58.
(3) Jankowiak, R.; Small, G. J. *Science* **1987**, *237*, 618.
(4) Friedrich, J.; Haarer, D. *Angew. Chem., Int. Ed. Engl.* **1984**, *23*, 113.
(5) Rebane, K. K.; Rebane, L. A. In *Persistent Spectral Hole-Burning: Science and Applications*; Moerner, W. E., Ed.; Springer-Verlag: Berlin, 1988; Vol. 44, p 17.
(6) Völker, S. *Annu. Rev. Phys. Chem.* **1989**, *40*, 499.
(7) Friedrich, J. In *Biochemical Spectroscopy*; Sauer, K., Ed.; Academic Press: San Diego, CA, 1995; Vol. 246, p 226.
(8) Reddy, N. R. S.; Lyle, P. A.; Small, G. J. *Photosynth. Res.* **1992**, *31*, 167.
(9) Thorn Leeson, D.; Wiersma, D. A.; Fritsch, K.; Friedrich, J. *J. Phys. Chem. B* **1997**, *101*, 6331.
(10) Reinot, T.; Zazubovich, V.; Hayes, J. M.; Small, G. J. *J. Phys. Chem. B* **2001**, *105*, 5083.
(11) Haarer, D. In *Persistent Spectral Hole-Burning: Science and Applications*; Moerner, W. E., Ed.; Springer-Verlag: Berlin, 1988; Vol. 44, p 79.
(12) Müller, K. P.; Haarer, D. *Phys. Rev. Lett.* **1991**, *66*, 2344.
(13) Schulte, G.; Grond, W.; Haarer, D.; Silbey, R. *J. Chem. Phys.* **1988**, *88*, 679.
(14) Maier, H.; Wunderlich, R.; Haarer, D.; Kharlamov, B. M.; Kulikov, S. G. *Phys. Rev. Lett.* **1995**, *74*, 5252.
(15) de Vries, H.; Wiersma, D. A. *Phys. Rev. Lett.* **1976**, *36*, 91.
(16) Gorokhovskii, A. A.; Kaarli, R. K.; Rebane, L. A. *JETP Lett.* **1974**, *20*, 216.
(17) Völker, S.; Macfarlane, R. M. *IBM J. Res. Dev.* **1979**, *23*, 547.
(18) Schellenberg, P.; Friedrich, J.; Kikas, J. *J. Chem. Phys.* **1994**, *101*, 9262.
(19) Johnson, M.; Orth, K.; Friedrich, J.; Trommsdorff, H. P. *J. Chem. Phys.* **1996**, *105*, 9762.
(20) Köhler, W.; Friedrich, J. *Europhys. Lett.* **1988**, *7*, 517.
(21) Friedrich, J.; Haarer, D.; Silbey, R. *Chem. Phys. Lett.* **1983**, *95*, 119.
(22) Friedrich, J. *Angew. Makromol. Chem.* **1990**, *183*, 115.
(23) Friebel, J.; Friedrich, J.; Suisalu, A.; Kikas, J.; Kuznetsov, A.; Laisaar, A.; Leiger, K. *J. Chem. Phys.* **1998**, *108*, 1830.
(24) Schellenberg, P.; Friedrich, J.; Kikas, J. *J. Chem. Phys.* **1994**, *100*, 5501.
(25) Gradl, G.; Feis, A.; Friedrich, J. *J. Chem. Phys.* **1992**, *97*, 5403.
(26) Ellervee, A.; Kikas, J.; Laisaar, A.; Shcherbakov, V.; Suisalu, A. *J. Opt. Soc. Am. B: Opt. Phys.* **1992**, *9*, 972.
(27) Sesselmann, T.; Richter, W.; Haarer, D.; Morawitz, H. *Phys. Rev. B* **1987**, *36*, 7601.
(28) Zollfrank, J.; Friedrich, J. *J. Opt. Soc. Am. B: Opt. Phys.* **1992**, *9*, 956.
(29) Köhler, W.; Friedrich, J. *Phys. Rev. Lett.* **1987**, *59*, 2199.
(30) Anderson, P. W.; Halperin, B. I.; Varma, C. M. *Philos. Mag.* **1972**, *25*, 1.
(31) Phillips, W. A. *J. Low Temp. Phys.* **1972**, *7*, 351.
(32) Hunklinger, S.; Raychaudhuri, A. K. In *Progress in Low Temperature Physics*; Brewer, D. F., Ed.; Elsevier: Amsterdam, 1986; Vol. IX, pp 265−344.
(33) Reinecke, T. L. *Solid State Commun.* **1979**, *32*, 1103.
(34) Kassner, K.; Silbey, R. *J. Phys. Condens. Matter* **1989**, *1*, 4599.
(35) Narasimhan, L. R.; Littau, K. A.; Pack, D. W.; Bai, Y. S.; Elschner, A.; Fayer, M. D. *Chem. Rev.* **1990**, *90*, 439.
(36) Somoza, M. M.; Friedrich, J.; Trommsdoff, H. P. *Chem. Phys. Lett.* **2006**, in press.
(37) Baudrand, J.; Walker, G. A. H. *PASP* **2001**, *113*, 851.
(38) Matsumoto, R.; Sakeda, K.; Matsushita, Y.; Suzuki, T.; Ichimura, T. *J. Mol. Struct.* **2005**, *735*−*36*, 153.
(39) Burland, D.; Haarer, D. *IBM J. Res. Dev.* **1979**, *23*, 534.
(40) Carpenter, G. B.; Halford, R. S. *J. Chem. Phys.* **1946**, *15*, 99.
(41) Burns, G.; Dacol, F. H. *Solid State Commun.* **1984**, *51*, 773.
(42) Trew, A. S.; Wilding, N. S.; Pawley, G. S. *Int. J. Mod. Phys. C* **1991**, *2*, 515.
(43) Wilding, N. B.; Crain, J.; Hatton, P. D.; Bushnellwye, G. *Acta Crystallogr. B* **1993**, *49*, 320.
(44) Crain, J.; Poon, W. C. K.; Cairnssmith, A.; Hatton, P. D. *J. Phys. Chem.* **1992**, *96*, 8168.
(45) Obremski, R. J.; Brown, C. W.; Lippincott, E. R. *J. Chem. Phys.* **1968**, *49*, 185.
(46) Plazanet, M.; Geis, A.; Johnson, M. R.; Trommsdoff, H. P. *J. Lumin.* **2002**, *98*, 197.
(47) Astilean, S.; Corval, A.; Casalegno, R.; Trommsdorff, H. P. *J. Lumin.* **1994**, *62*, 245.
(48) Zollfrank, J.; Friedrich, J. *J. Chem. Phys.* **1990**, *93*, 8586.
(49) Grannan, E. R.; Randeria, M.; Sethna, J. P. *Phys. Rev. B* **1990**, *41*, 7784.